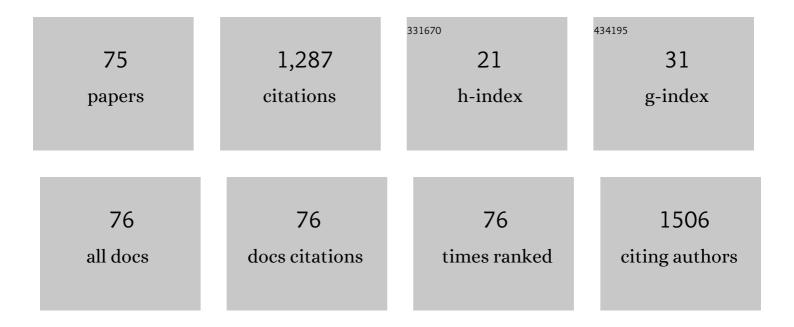
List of Publications by Year in descending order

Source: https://exaly.com/author-pdf/2362320/publications.pdf Version: 2024-02-01



#	Article	IF	CITATIONS
1	High thermoelectric figure-of-merits from large-area porous silicon nanowire arrays. Nano Energy, 2015, 13, 433-441.	16.0	95
2	Designing a Transparent CdIn <sub>2</sub> S <sub>4</sub> /In <sub>2</sub> S <sub>3</sub> Bulkâ€Heterojunction Photoanode Integrated with a Perovskite Solar Cell for Unbiased Water Splitting. Advanced Materials, 2020, 32, e2002893.	21.0	67
3	Modulating oxygen vacancies in Sn-doped hematite film grown on silicon microwires for photoelectrochemical water oxidation. Journal of Materials Chemistry A, 2018, 6, 15593-15602.	10.3	53
4	Thermodynamic loss mechanisms and strategies for efficient hot-electron photoconversion. Nano Energy, 2019, 55, 164-172.	16.0	50
5	Facile morphological control of single-crystalline silicon nanowires. Applied Surface Science, 2012, 258, 9792-9799.	6.1	39
6	Perovskite Solar Cells: Optoelectronic Simulation and Optimization. Solar Rrl, 2018, 2, 1800126.	5.8	39
7	Strong and highly asymmetrical optical absorption in conformal metal-semiconductor-metal grating system for plasmonic hot-electron photodetection application. Scientific Reports, 2015, 5, 14304.	3.3	36
8	Nanowire and nanohole silicon solar cells: a thorough optoelectronic evaluation. Progress in Photovoltaics: Research and Applications, 2015, 23, 1734-1741.	8.1	35
9	Surface Morphology-Dependent Photoelectrochemical Properties of One-Dimensional Si Nanostructure Arrays Prepared by Chemical Etching. ACS Applied Materials & Interfaces, 2013, 5, 4769-4776.	8.0	34
10	Optoelectronic modeling of the Si/α-Fe2O3 heterojunction photoanode. Nano Energy, 2018, 43, 177-183.	16.0	34
11	Photonic surface waves enabled perfect infrared absorption by monolayer graphene. Nano Energy, 2018, 48, 161-169.	16.0	33
12	Regulating the Silicon/Hematite Microwire Photoanode by the Conformal Al <sub>2</sub> O <sub>3</sub> Intermediate Layer for Water Splitting. ACS Applied Materials & Interfaces, 2019, 11, 5978-5988.	8.0	33
13	High-efficiency photon capturing in ultrathin silicon solar cells with front nanobowl texture and truncated-nanopyramid reflector. Optics Letters, 2015, 40, 1077.	3.3	31
14	Facile Preparation of <i>n</i> â€Type LaFeO <sub>3</sub> Perovskite Film for Efficient Photoelectrochemical Water Splitting. ChemistrySelect, 2018, 3, 968-972.	1.5	29
15	Field emission enhancement of Au-Si nano-particle-decorated silicon nanowires. Nanoscale Research Letters, 2011, 6, 176.	5.7	28
16	Infrared hot-carrier photodetection based on planar perfect absorber. Optics Letters, 2015, 40, 4261.	3.3	28
17	Omnidirectional absorption enhancement of symmetry-broken crescent-deformed single-nanowire photovoltaic cells. Nano Energy, 2015, 13, 9-17.	16.0	26
18	Significant reduction of thermal conductivity in silicon nanowire arrays. Nanotechnology, 2013, 24, 505718.	2.6	25

#	Article	IF	CITATIONS
19	Planar dual-cavity hot-electron photodetectors. Nanoscale, 2019, 11, 1396-1402.	5.6	24
20	Improved optical absorption of silicon single-nanowire solar cells by off-axial core/shell design. Nano Energy, 2015, 17, 233-240.	16.0	23
21	Narrowband and Full-Angle Refractive Index Sensor Based on a Planar Multilayer Structure. IEEE Sensors Journal, 2019, 19, 2924-2930.	4.7	23
22	Surface-plasmon enhanced photodetection at communication band based on hot electrons. Journal of Applied Physics, 2015, 118, .	2.5	22
23	Tunable light absorbance by exciting the plasmonic gap mode for refractive index sensing. Optics Letters, 2018, 43, 1427.	3.3	22
24	Tin and Oxygen-Vacancy Co-doping into Hematite Photoanode for Improved Photoelectrochemical Performances. Nanoscale Research Letters, 2020, 15, 54.	5.7	22
25	Plasmon gap mode-assisted third-harmonic generation from metal film-coupled nanowires. Applied Physics Letters, 2014, 104, .	3.3	21
26	Simultaneously performing optical and electrical responses from a plasmonic sensor based on gold/silicon Schottky junction. Optics Express, 2019, 27, 38382.	3.4	21
27	Design of dual-diameter nanoholes for efficient solar-light harvesting. Nanoscale Research Letters, 2014, 9, 481.	5.7	19
28	Irradiation Damage Determined Field Emission of Ion Irradiated Carbon Nanotubes. ACS Applied Materials & Interfaces, 2014, 6, 5137-5143.	8.0	18
29	Si microwire array photoelectrochemical cells: Stabilized and improved performances with surface modification of Pt nanoparticles and TiO2 ultrathin film. Journal of Power Sources, 2017, 342, 460-466.	7.8	18
30	Tunable infrared hot-electron photodetection by exciting gap-mode plasmons with wafer-scale gold nanohole arrays. Optics Express, 2020, 28, 6511.	3.4	18
31	Constructing a full-space internal electric field in a hematite photoanode to facilitate photogenerated-carrier separation and transfer. Journal of Materials Chemistry A, 2022, 10, 8546-8555.	10.3	17
32	Gap-mode excitation, manipulation, and refractive-index sensing application by gold nanocube arrays. Nanoscale, 2019, 11, 5467-5473.	5.6	16
33	Self-improvement of solar water oxidation for the continuously-irradiated hematite photoanode. Dalton Transactions, 2019, 48, 15151-15159.	3.3	15
34	Enhanced photoabsorption in front-tapered single-nanowire solar cells. Optics Letters, 2014, 39, 5756.	3.3	14
35	Enhanced Photoresponsivity of a Germanium Single-Nanowire Photodetector Confined within a Superwavelength Metallic Slit. ACS Photonics, 2014, 1, 483-488.	6.6	14
36	Stabilized and Improved Photoelectrochemical Responses of Silicon Nanowires Modified with Ag@SiO <sub>2</sub> Nanoparticles and Crystallized TiO <sub>2</sub> Film. ACS Applied Materials & Interfaces, 2016, 8, 30072-30078.	8.0	14

#	Article	IF	CITATIONS
37	Photoelectrochemical responses of silicon nanowire arrays for light detection. Chemical Physics Letters, 2012, 538, 102-107.	2.6	13
38	Size-dependent performances in homogeneous, controllable, and large-area silicon wire array photocathode. Journal of Power Sources, 2020, 473, 228580.	7.8	13
39	Nanobowls-assisted broadband absorber for unbiased Si-based infrared photodetection. Optics Express, 2021, 29, 15505.	3.4	13
40	Reconstructing Oxygen Vacancies in the Bulk and Nickel Oxyhydroxide Overlayer to Promote the Hematite Photoanode for Photoelectrochemical Water Oxidation. ACS Applied Energy Materials, 2022, 5, 8999-9008.	5.1	13
41	Diamond-like carbon decoration enhances the field electron emission of silicon nanowires. Surface and Coatings Technology, 2013, 228, S349-S353.	4.8	12
42	Design of μc-Si:H/a-Si:H coaxial tandem single-nanowire solar cells considering photocurrent matching. Optics Express, 2014, 22, A1761.	3.4	12
43	Coaxial Ag/ZnO/Ag nanowire for highly sensitive hot-electron photodetection. Applied Physics Letters, 2015, 106, 081109.	3.3	12
44	Facile fabrication of wafer-scale, micro-spacing and high-aspect-ratio silicon microwire arrays. RSC Advances, 2016, 6, 87486-87492.	3.6	12
45	Planar, narrowband, and tunable photodetection in the near-infrared with Au/TiO <sub>2</sub> nanodiodes based on Tamm plasmons. Nanoscale, 2019, 11, 23182-23187.	5.6	12
46	Underlayer engineering into the Sn-doped hematite photoanode for facilitating carrier extraction. Physical Chemistry Chemical Physics, 2020, 22, 7306-7313.	2.8	12
47	Tunable synthesis of carbon nanosheet/silicon nanowire hybrids for field emission applications. Diamond and Related Materials, 2012, 26, 83-88.	3.9	11
48	Absorption enhancement of single silicon nanowire by tailoring rear metallic film for photovoltaic applications. Optics Letters, 2014, 39, 817.	3.3	11
49	Limiting efficiency calculation of silicon single-nanowire solar cells with considering Auger recombination. Applied Physics Letters, 2015, 106, .	3.3	10
50	Understanding the varying mechanisms between the conformal interlayer and overlayer in the silicon/hematite dual-absorber photoanode for solar water splitting. Dalton Transactions, 2021, 50, 2936-2944.	3.3	10
51	Tunable multi-wavelength polymer laser based on a triangular-lattice photonic crystal structure. Journal Physics D: Applied Physics, 2016, 49, 335103.	2.8	8
52	Fabricating vertically aligned ultrathin graphene nanosheets without any catalyst using rf sputtering deposition. Nuclear Instruments & Methods in Physics Research B, 2013, 307, 177-180.	1.4	7
53	Enhanced Photoelectrochemical Response of Silicon Nanowire Arrays through Coating the Carbon Shell. Journal of the Electrochemical Society, 2014, 161, H240-H243.	2.9	7
54	All-organic room temperature thermally switchable dielectric system. Journal of Materials Chemistry C, 2019, 7, 15315-15321.	5.5	6

#	Article	IF	CITATIONS
55	Morphology-dependent optical properties of one-dimensional nanostructure-arrayed silicon. Journal of the Korean Physical Society, 2013, 63, 1189-1193.	0.7	5
56	Performance-improved thin-film a-Si:H/μc-Si:H tandem solar cells by two-dimensionally nanopatterning photoactive layer. Nanoscale Research Letters, 2014, 9, 73.	5.7	5
57	Simulation Analysis on Photoelectric Conversion Characteristics of Silicon Nanowire Array Photoelectrodes. Nanoscale Research Letters, 2015, 10, 985.	5.7	4
58	Proximity effect assisted absorption enhancement in thin film with locally clustered nanoholes. Optics Letters, 2015, 40, 792.	3.3	4
59	Direct growth of hematite film on p+n-silicon micro-pyramid arrays for low-bias water splitting. Solar Energy Materials and Solar Cells, 2021, 224, 110987.	6.2	4
60	Photo-assisted decoration of Ag-Pt nanoparticles on Si photocathodes for reducing overpotential toward enhanced photoelectrochemical water splitting. Science China Materials, 2022, 65, 3033-3042.	6.3	4
61	Back Interface Passivation for Efficient Low-Bandgap Perovskite Solar Cells and Photodetectors. Nanomaterials, 2022, 12, 2065.	4.1	3
62	Enhanced Light Trapping in a-Si:H/μc-Si:H Tandem Solar Cells via Nanopatterning Top Absorber and Embedding Wavelength-Selective Intermediate Reflectors. IEEE Journal of Photovoltaics, 2015, 5, 46-54.	2.5	2
63	Physical manipulation of ultrathin-film optical interference for super absorption and two-dimensional heterojunction photoconversion. Chinese Physics B, 2018, 27, 124202.	1.4	2
64	Structures and Field Emission Properties of Silicon Nanowire Arrays Implanted with Energetic Carbon Ion Beam. Journal of Nanoscience and Nanotechnology, 2012, 12, 6543-6547.	0.9	1
65	H plasma processing triggered phase transformation from DLC to diamond nano-particles. Diamond and Related Materials, 2012, 25, 45-49.	3.9	1
66	A mechanically bendable and conformally attachable polymer membrane microlaser array enabled by digital interference lithography. Nanoscale, 2020, 12, 6736-6743.	5.6	1
67	Planar Narrowband Hot-Electron Photodetector Based on Tamm Plasmons. , 2019, , .		1
68	Numerical Simulations of Optical Absorption and Spectral Selective of Ni Nanowire/AAO Composites. Key Engineering Materials, 2014, 602-603, 975-979.	0.4	0
69	Study on limiting efficiencies of a-Si:H/μc-Si:H-based single-nanowire solar cells under single and tandem junction configurations. Applied Physics Letters, 2015, 107, 181106.	3.3	0
70	Optoelectronic and thermodynamic simulation of solar cells. , 2016, , .		0
71	Design and fabrication of silicon immersion grating. , 2021, , .		0
72	Selective optical sensing of glucose based on ordered nanowires/disordered porous Si hybrid structure. , 2021, , .		0

#	Article	IF	CITATIONS
73	Planar Dual-Layer System for Ultra-Broadband Absorption and Hot-Carrier Photodetection in Longwave Near-Infrared Band. IEEE Journal of Selected Topics in Quantum Electronics, 2022, 28, 1-9.	2.9	0
74	Influences of Metal Nanoparticles on the Photoelectrochemical Activity of Silicon Nanowires for Photon Harvesting. , 2015, , .		0
75	Unity integration of Au grating and microfluid for refractive-index sensing. , 2020, , .		0